

## Fano Profiles Induced by Near-Field Coupling in Heterogeneous Dimers of Gold and Silver Nanoparticles

G. Bachelier, I. Russier-Antoine, E. Benichou, C. Jonin, N. Del Fatti, F. Vallée, and P.-F. Brevet

*Laboratoire de Spectrométrie Ionique et Moléculaire, Université Lyon 1-CNRS (UMR 5579),*

*43 Boulevard du 11 Novembre 1918, 69622 Villeurbanne Cedex, France*

(Received 28 April 2008; published 4 November 2008)

The near-field coupling between a gold and a silver spherical nanoparticle is investigated theoretically. Fano profiles are observed in the absorption cross section of the gold nanoparticle due to the coupling between the spectrally localized surface plasmon resonance of the silver nanoparticle and the continuum of interband transitions of the gold one. The effect of dimer internal characteristics (particle sizes and distance), surrounding medium (through the refractive index), and external excitation (polarization and propagation directions) are addressed. In particular, it is shown that the near-field coupling can be tuned from the weak to the strong regime by rotating the polarization direction, and that the Fano profiles are sensitive to the shadowing effect even for small particle sizes.

DOI: 10.1103/PhysRevLett.101.197401

PACS numbers: 78.67.Bf, 42.25.Fx, 73.20.Mf, 73.22.-f

Scaling down the size of noble metal structures has opened an extensively productive road to manipulate light at a subwavelength scale. The shape-driven frequency of the surface plasmon resonances (SPR) allows the tailoring of almost any desired spectral response in the visible and the near infrared domains, depending on the targeted applications [1]. Another powerful strategy, the focus of a large and increasing interest in plasmonics, lies in the interparticle near-field coupling through the evanescent waves surrounding the metal nanostructures. Bonding and antibonding plasmon modes, in a hybridization picture [2], strongly depend on the particle distance [3–5] and eventually lead to a singular response in the limit of contacting dimers [6]. Controlling the nanoparticle spacing is therefore a major challenge achieved using either physical or chemical techniques [3,7–10]. The large electric field localized in the dimer gap is indeed a key ingredient used to induce surface enhanced Raman scattering [11], single molecule fluorescence [12], or frequency mixing [10] with a single homogeneous dimer. Additional effects such as radiation damping modification [13] and enhanced optical forces [14] have also been predicted, underlying the wide interest in coupled metal structures.

Fano profiles are typical spectral features arising from the coupling of a discrete state with a continuum [15]. They have been reported in the past for  $J$ -aggregated Dye or semiconductor quantum dots (discrete exciton) coupled with gold nanoparticles (continuum) [16,17]. In these systems, the SPR of the noble metal particles was used to enhance the response of the coupled system, but does not play any key role in the observation of the Fano profiles. Fano-like line shapes were also reported recently in reflection spectra of interacting metal nanowires made of the same metal, but their origin was assigned to the interference between the light scattered by (noninteracting) sub-radiant and superradiant plasmon modes [18]. In this Letter

we investigate theoretically the optical properties of heterogeneous dimers composed of a gold and a silver nanoparticle. We demonstrate for the first time the presence of Fano profiles in a purely plasmonic system, where the spectrally localized SPR of the silver nanoparticle (the “discrete” level) is coupled to the gold interband transitions (the continuum). These characteristic spectral features are revealed in the absorption spectrum of the gold nanoparticle, and their sensitivity on the dimer structure, the surrounding medium, and the excitation configuration is addressed.

When the excitation wavelength largely exceeds the particle size, the optical properties of noble metal nanoparticles are dominated by absorption [1]. The latter is quantified by a normalized cross section  $Q_{\text{abs}} = \sigma_{\text{abs}}/S$  weighting the Joule dissipation inside the particle with respect to the incident power intercepted by the particle:

$$Q_{\text{abs}} = \frac{\int \mathbf{j} \cdot \mathbf{E} dV}{\int \mathbf{E}_i \times \mathbf{H}_i dS}. \quad (1)$$

$\mathbf{E}$  and  $\mathbf{j}$  are the total electric field and charge currents inside the particle, and  $\mathbf{E}_i$  and  $\mathbf{H}_i$  account for the incident electric and magnetic fields.  $V$  and  $S$  are the particle volume and the particle section normal to the incident wave, respectively. In this work, the adimensional quantity  $Q_{\text{abs}}$  was computed for the gold and silver particles in the heterogeneous dimer using finite element method (FEM) simulations performed in the framework of the scattered field formulation. Perfectly matched layers were used to avoid spurious reflections at the surrounding medium boundaries [19]. The dielectric constants of the metal particles  $\epsilon_p$  were taken from Ref. [20], and corrected, for small particle sizes, to account for the Landau damping of the SPR [21]. The results are shown in Fig. 1 for particle radii  $R$  and a distance  $d$  (surface to surface) of 5 and 3 nm, respectively. The refractive index of the surrounding me-

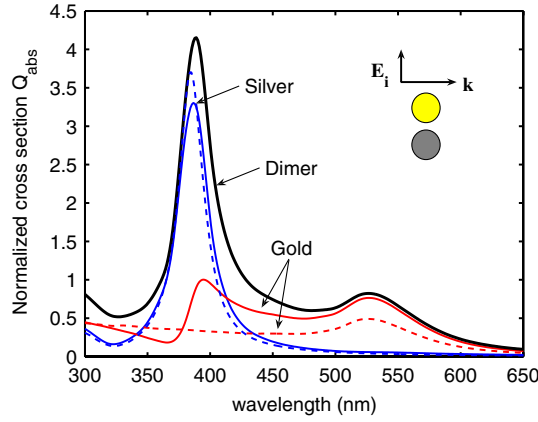


FIG. 1 (color online). Normalized absorption cross sections of the silver and gold nanoparticles. The dashed and full lines correspond to the case of isolated particles or particles within the dimer, respectively. The overall absorption cross section of the coupled particles is given by the bold line. The radius of both particles is 5 nm and the interparticle distance 3 nm. The incoming light is polarized parallel to the dimer axis. The gold and the silver particles are represented by the light gray and the gray disks, respectively.

dium ( $\sqrt{\epsilon_m}$ ) is fixed at 1.33. As observed in Fig. 1, the SPR of the silver nanoparticle is only slightly damped and shifted in the heterogeneous dimer (the increase of the width and the resonance wavelength shift are smaller than 3 nm). On the opposite, the absorption in the gold particle is highly modified in the overall spectral range covered by the simulations. In particular, a clear Fano profile is observed in the gold particle around 378 nm induced by the near-field coupling between the continuum of interband transitions in the gold material and the discrete SPR of the silver particle. More precisely, the interband transitions of the gold particle can be excited either directly by the light source or indirectly through the locally enhanced electric field associated with the SPR of the silver particle. The relative phase between the incident field and that scattered by the silver particle therefore plays a major role. The origin of this phase shift can be qualitatively understood using the particle polarizability  $\alpha$  in the Rayleigh approximation [1]

$$\alpha = 4\pi R^3 \frac{\epsilon_p - \epsilon_m}{\epsilon_p + 2\epsilon_m}. \quad (2)$$

The real part of  $\epsilon_p$  being negative around the SPR, observed for  $\text{Re}(\epsilon_p + 2\epsilon_m) = 0$ , the dipole induced in the silver particle is in phase with the incident electric field below the SPR (longer wavelengths) and out of phase above the SPR, as given by the sign of the real part of the denominator.

The intrinsic near-field origin of the particle coupling leads to a strong dependence of the Fano profile with the particle distance  $d$  as shown in Fig. 2(a). For large distances (greater than the particle diameter), the profiles are almost antisymmetric with respect to the crossing point of

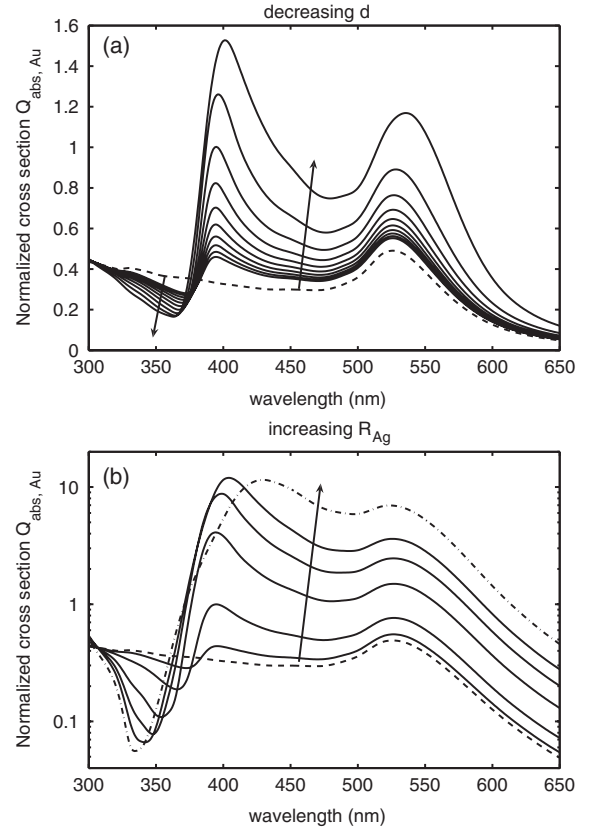


FIG. 2. Normalized absorption cross section of a  $R_{Au} = 5$  nm gold nanoparticle (a) as a function of the interparticle distance  $d$  (from top to bottom  $d$  ranges from 1 to 10 nm by steps of 1 nm) for a fixed silver size ( $R_{Ag} = 5$  nm) and (b) as a function of silver particle size (from the bottom to the top  $R_{Ag} = 2.5, 5, 10, 15, 20,$  and  $30$  nm) for a fixed interparticle distance  $d = 3$  nm. The dash-dotted line is used for  $R_{Ag} = 30$  nm. The dashed curves correspond to the absorption cross section of an isolated gold particle. The field configuration is the same as in Fig. 1.

the normalized cross section  $Q_{abs,Au}^\infty$  calculated for an isolated particle and  $Q_{abs,Au}$  for the gold particle in the heterogeneous dimer. For shorter distances, the Fano profiles are highly distorted showing the continuous transition from the weak to the strong coupling regime [15]. The same behavior is observed in Fig. 2(b) while increasing the silver particle radius. Indeed, for noble metal nanospheres, the near-field region typically extends over one particle radius [1]. Increasing the silver particle radius  $R_{Ag}$  allows us, therefore, to adjust the region of localized and enhanced electric field to the gold nanoparticle size. As a matter of fact, with  $R_{Au} = 5$  nm, an optimum was found for  $R_{Ag} \approx 2R_{Au} + d$ . For larger  $R_{Ag}$ , the enhancement of the normalized cross section  $Q_{abs,Au}$  saturates due to the retardation effects on the silver particle, leading to a shift and a radiative broadening of its SPR [see the dash-dotted curve of Fig. 2(b)].

If the gold absorption cross section is spectrally highly affected by the presence of the silver SPR, an almost

constant and comparable enhancement is found for longer wavelengths, as shown in Figs. 2(a) and 2(b). This unusual behavior is at variance with the common picture of local field enhancement used in surface enhanced Raman scattering, for example [11], where a significant enhancement is expected only close to the SPR. For weakly interacting particles [ $d > \max(R_{\text{Au}}, R_{\text{Ag}})$ ], the field enhancement deduced from the FEM simulations is in good agreement with that calculated analytically, using the dipolar approximation for the field scattered by the silver particle

$$\mathbf{E}_{s,\text{Ag}} = \frac{1}{4\pi\epsilon_0\epsilon_m r^3} [3(\mathbf{p}_{\text{Ag}} \cdot \mathbf{e}_r)\mathbf{e}_r - \mathbf{p}_{\text{Ag}}]. \quad (3)$$

$r$  and  $\mathbf{e}_r$  are the distance and the direction from the localized dipole,  $\mathbf{p}_{\text{Ag}} = \epsilon_0\epsilon_m\alpha_{\text{Ag}}\mathbf{E}_i$ , to the point where the field is evaluated. The relatively weak enhancement at the silver SPR is indeed due to the large distance between the particle center ( $r = d + R_{\text{Au}} + R_{\text{Ag}}$ ), and the constant value of the enhancement below the silver SPR (longer wavelengths) simply arises from the polarizability  $\alpha$ , which is almost independent of the wavelength ( $|\epsilon_p| \gg |\epsilon_m|$ ). In the strong coupling regime [ $d < \max(R_{\text{Au}}, R_{\text{Ag}})$ ], the optical properties of the silver particle are significantly modified, so that the previous approach is no longer valid and leads to a largely overestimated enhancements around the silver SPR.

The effects of the surrounding medium, through its dielectric constant  $\epsilon_m$ , on the Fano profiles were also studied (data not shown here). Since the normalized cross section for an isolated particle

$$Q_{\text{abs,Au}}^{\infty} = \frac{k}{\pi R_{\text{Au}}^2} \text{Im}(\alpha_{\text{Au}}) \quad (4)$$

already depends on  $\epsilon_m$  through both the wave vector  $k$  in the surrounding medium and the polarizability  $\alpha_{\text{Au}}$  [1], the obtained results for the heterogeneous dimer  $Q_{\text{abs,Au}}$  were normalized by  $Q_{\text{abs,Au}}^{\infty}$ . Doing so,  $Q_{\text{abs,Au}}/Q_{\text{abs,Au}}^{\infty}$  was found to be almost independent of  $\epsilon_m$  (and approx. equal to 1.5) below the silver SPR (longer wavelengths) for  $R = 5$  nm,  $d = 3$  nm, and  $\epsilon_m$  ranging from 1 to 2. In contrast, the Fano profiles in  $Q_{\text{abs,Au}}/Q_{\text{abs,Au}}^{\infty}$  are frequency shifted, following the SPR of the silver particle, and enhanced as  $\epsilon_m$  is increased. Those observations can be explained by the  $\epsilon_m$  dependence of the field scattered by the silver nanoparticle  $\mathbf{E}_{s,\text{Ag}}$  [cf. Eq. (3)]. The latter is directly proportional to the polarizability  $\alpha_{\text{Ag}}$  (through  $\mathbf{p}_{\text{Ag}}$ ), which is almost independent of  $\epsilon_m$  for long wavelengths and strongly depends on  $\epsilon_m$  close to the silver SPR, as expected.

As shown by Eq. (3), the dephasing between the incident and the scattered field, responsible for the observed Fano profiles, not only depends on the polarizability of the silver particle (included in  $\mathbf{p}_{\text{Ag}}$ ). It also depends on the relative orientation of the dimer axis (along  $\mathbf{e}_r$ ) with respect to the incident field (parallel to  $\mathbf{p}_{\text{Ag}}$ ). The results obtained by the

FEM simulations are shown in Fig. 3 where the angle  $\gamma$  between the incident field  $\mathbf{E}_i$  and the dimer axis is varied from 0 to  $\pi/2$ . A clear phase shift is observed together with a reduction of the Fano profile amplitude, as expected from Eq. (3). Hence, in a hybridization picture [2], the coupling parameter between the two particles can be easily adjusted by rotating the polarization angle, allowing us to externally control the coupling regime from the weak to the strong limit.

Interestingly, all curves of Fig. 3 cross in a single point around 381 nm. This can be understood if one keeps in mind that only two eigenmodes of the heterogeneous dimer can be excited (at  $\gamma = 0$  and  $\gamma = \pi/2$ ) in the configuration of Fig. 3. Hence, the dimer response is a linear combination of the two eigenmode responses, leading to an isobestic point (independent of  $\gamma$ ) where the two curves corresponding to  $\gamma = 0$  and  $\gamma = \pi/2$  crosses. A striking consequence is that  $Q_{\text{abs,Au}}$  is larger than  $Q_{\text{abs,Au}}^{\infty}$  whatever (i) the incident polarization at the isobestic point and (ii) the incident wavelength for a particular value of  $\gamma$  (here  $\gamma = \pi/3$ ), as shown by the intermediate bold curve of Fig. 3. The latter case can be surprising at first glance from Eq. (3), owing to the phase shift of  $\alpha_{\text{Ag}}$ , and hence of  $\mathbf{p}_{\text{Ag}}$ , while going from one side to the other of the silver SPR spectrum. This singular behavior arises when the scattered field  $\mathbf{E}_{s,\text{Ag}}$  experienced by the gold particle is perpendicular to the incident field  $\mathbf{E}_i$  [the corresponding value of  $\gamma$  can be obtained by setting  $\mathbf{E}_{s,\text{Ag}} \cdot \mathbf{E}_i = 0$  in Eq. (3)]. In that case, the rms amplitude of the electric field experienced by the gold particle,  $\propto (|E_{s,\text{Ag}}|^2 + |E_i|^2)^{1/2}$ , is always larger than that of the incident field,  $\propto |E_i|$ , whatever the phase of  $\alpha_{\text{Ag}}$ .

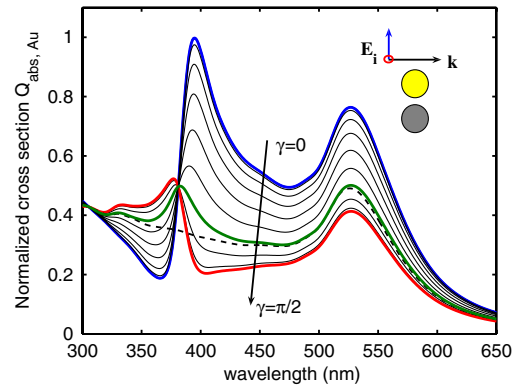


FIG. 3 (color online). Normalized absorption cross section of a  $R = 5$  nm gold nanoparticle as a function of the angle  $\gamma$  between the incoming electric field and the dimer axis (the wave vector is perpendicular to the dimer axis). The bold lines from top to bottom (as indicated by the arrow) correspond to  $\gamma = 0$ ,  $\pi/3$ , and  $\pi/2$ , respectively. For the thin lines,  $\gamma$  increases by steps of 10 degrees. The dashed curves correspond to the absorption cross section of an isolated gold particle. The radius of the silver nanoparticle is 5 nm and the interparticle distance 3 nm.

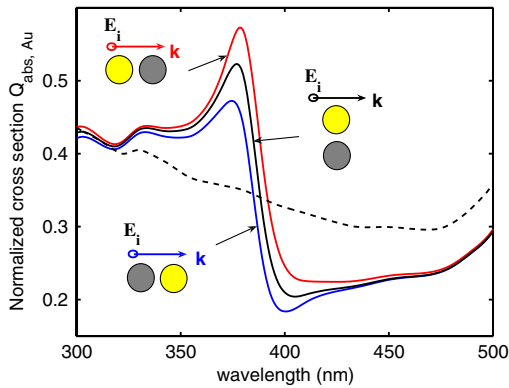


FIG. 4 (color online). Normalized absorption cross section of a  $R = 5$  nm gold nanoparticle as a function of the orientation of the dimer with respect to the incoming wave vector. The light gray and gray disks correspond to the gold and silver particles, respectively. The incoming electric field is always perpendicular to the dimer axis ( $\gamma = \pi/2$ ) and the dashed curves correspond to the absorption cross section of an isolated gold particle.

Finally, we would like to discuss the influence of the incidence angle with respect to the dimer axis. In order to decouple this effect from that of the polarization angle  $\gamma$ , the dimer axis  $\mathbf{e}_d$  was chosen perpendicular to  $\mathbf{E}_i$  in all cases. Following Eq. (3), the electric field  $\mathbf{E}_{s,Ag}$  scattered by the silver particle in the dipolar approximation is therefore parallel to  $\mathbf{E}_i$  and of constant amplitude whatever the dimer orientation [the first term in brackets of Eq. (3) cancels out]. Hence, in this simple model, no particular effect is expected while rotating the heterogeneous dimer. This is at variance with the results of the FEM simulations reported in Fig. 4. The dependence of the absorption in the gold particle on the orientation of the dimer is a signature of the “shadowing” effect, observed here despite the small nanoparticles size with respect to the wavelength ( $R = 5$  nm). This shadowing effect, not present in Eq. (3), is sensitive only close to the silver SPR. It is therefore a direct consequence of the strong coupling regime due to the large field enhancement associated with the silver SPR. Note that the dimer orientation leads to a global increase or decrease of the normalized absorption cross section  $Q_{abs,Au}$ , in contrast with the effect of polarization shown in Fig. 3. Therefore, a precise investigation of the absorption in the gold nanoparticle allows in principle to determine the 3D orientation of the heterogeneous dimer, owing to its noncentrosymmetry.

In conclusion, we have explored theoretically the linear optical properties of a heterogeneous dimer composed of a gold and a silver nanoparticle. Fano profiles in the absorption of the gold nanoparticle have been evidenced due to the near-field coupling between the silver SPR and the gold interband transitions. It is shown that (i) the Fano profiles are strongly enhanced while decreasing the gap between the particles and the ratio  $R_{Au}/R_{Ag}$  until the gold nanoparticle is fully included in the near-field region of the silver particle, (ii) the enhancement of the gold nanopar-

ticle absorption is large not only close to the silver SPR but also for longer wavelengths where it is found to be constant, (iii) it is possible to externally control the coupling regime by rotating the incident polarization, and (iv) the orientation of the heterogeneous dimer can be determined using the shadowing effect, even for particles small compared to the wavelength. The experimental observation of the Fano profiles in heterogeneous dimers is challenging using linear spectroscopy since they are hardly visible on the absorption spectra of the dimers. However, they could be easily observable by nonlinear spectroscopy, using for instance two-color femtosecond pump-probe approach to excite the dimer and selectively probe its gold component.

- [1] C.F. Bohren and D.R. Huffman, *Absorption and Scattering of Light by Small Particles* (Wiley Interscience, New York, 1983); U. Kreibig and M. Vollmer, *Optical Properties of Metal Clusters* (Springer, Berlin, 1995).
- [2] P. Nordlander, C. Oubre, E. Prodan, K. Li, and M.I. Stockman, *Nano Lett.* **4**, 899 (2004).
- [3] L. Gunnarsson, T. Rindzevicius, J. Prikulis, B. Kasemo, M. Kall, S.L. Zou, and G.C. Schatz, *J. Phys. Chem. B* **109**, 1079 (2005).
- [4] O.L. Muskens, V. Giannini, J.A. Sanchez-Gil, and J.G. Rivas, *Opt. Express* **15**, 17736 (2007).
- [5] P. Billaud *et al.*, *J. Phys. Chem. C* **112**, 978 (2008).
- [6] I. Romero, J. Aizpurua, G.W. Bryant, and F.J.G. de Abajo, *Opt. Express* **14**, 9988 (2006).
- [7] R. Sardar, T.B. Heap, and J.S. Shumaker-Parry, *J. Am. Chem. Soc.* **129**, 5356 (2007).
- [8] P. Ahonen, D.J. Schiffrin, J. Paprotny, and K. Kontturi, *Phys. Chem. Chem. Phys.* **9**, 651 (2007).
- [9] M. Ringler *et al.*, *Nano Lett.* **7**, 2753 (2007).
- [10] M. Danckwerts and L. Novotny, *Phys. Rev. Lett.* **98**, 026104 (2007).
- [11] C.E. Talley, J.B. Jackson, C. Oubre, N.K. Grady, C.W. Hollars, S.M. Lane, T.R. Huser, P. Nordlander, and N.J. Halas, *Nano Lett.* **5**, 1569 (2005).
- [12] J. Zhang, Y. Fu, M.H. Chowdhury, and J.R. Lakowicz, *Nano Lett.* **7**, 2101 (2007).
- [13] C. Dahmen, B. Schmidt, and G. von Plessen, *Nano Lett.* **7**, 318 (2007).
- [14] A.S. Zelenina, R. Quidant, and M. Nieto-Vesperinas, *Opt. Lett.* **32**, 1156 (2007).
- [15] U. Fano, *Phys. Rev.* **124**, 1866 (1961).
- [16] A.M. Kelley, *Nano Lett.* **7**, 3235 (2007).
- [17] W. Zhang, A.O. Govorov, and G.W. Bryant, *Phys. Rev. Lett.* **97**, 146804 (2006).
- [18] A. Christ, Y. Ekinici, H.H. Solak, N.A. Gippius, S.G. Tikhodeev, and O.J.F. Martin, *Phys. Rev. B* **76**, 201405 (R) (2007).
- [19] J. Jin, *The Finite Elements Method in Electrodynamics* (Wiley Interscience, New York, 2002).
- [20] P.B. Johnson and R.W. Christy, *Phys. Rev. B* **6**, 4370 (1972).
- [21] R.A. Molina, D. Weinmann, and R.A. Jalabert, *Phys. Rev. B* **65**, 155427 (2002).